FIRST SEMI-ANNUAL PROGRESS REPORT

NASA GRANT NAG8-950

CONVECTIVE FLOW EFFECTS ON PROTEIN CRYSTAL GROWTH

Period of Performance
2/1/93 through 7/31/93

Principal Investigator
FRANZ ROSENBERGER

Co-Investigator
LISA A. MONACO

Center for Microgravity and Materials Research
University of Alabama in Huntsville
Huntsville, Alabama 35899

Summary of Work Performed

The experimental setup for the in-situ high resolution optical monitoring of protein crystal growth/dissolution morphologies has been substantially improved. By augmenting the observation system with a temperature-controlled enclosure, laser illumination for the interferometric microscope, and software for pixel by pixel light intensity recording, a height resolution of about two unit cells for lysozyme can now be obtained.

The repartitioning of Na^+ and Cl^- ions between lysozyme solutions and crystals was studied. Quite unexpectedly, it was found that the longer crystals were in contact with their solution, the lower was their ion content.

The development of a model for diffusive-convective transport and resulting distribution of the growth rate on facets has been completed. Results obtained for a realistic growth cell geometry show interesting differences between "growth runs" at 1g and 0g.

The kinematic viscosity of lysozyme solutions of various supersaturations and salt concentrations was monitored over time. In contrast to the preliminary finding of other authors, we found no changes in viscosity over four days.

The experimental setup for light scattering investigations of aggregation and nucleation in protein solutions has been completed, and a computer program for the evaluation of multi-angle light scattering data was acquired.

Table of Contents

1. Introduction

Our main research objectives under this grant are:

1. To investigate the effect(s) of defined convective transport and supersasturation conditions on the growth kinetics and morphology of selected proteins.
2. To establish a correlation between the growth conditions and x-ray diffraction resolution for some of the proteins investigated.

As outlined in the original proposal, these objectives are to be pursued through work on the following tasks:

1. Refinement of our earlier morphology and kinetics studies without forced flow. The high-resolution morphology results obtained will serve as reference cases for the forced flow studies. In particular, this will be a continuation of our investigations of lysozyme
2. Kinetics studies under forced flow
3. Determination of the repartitioning of the precipitant between solution and crystal
4. Numerical modelling of diffusive-convective transport
5. Preparation, purification and compositional analysis of proteins
6. Diffusivity measurements
7. Kinematic viscosity measurements
8. Protein aggregation/nucleation studies
9. X-ray diffraction resolution determinations

2. Work Performed

During the report period, work was performed on tasks 1, 3, 4, 7 and 8. Details are given in the following Sections.

2.1. Refinement of Morphology and Kinetics Studies Without Forced Flow

The aim of this work is twofold:

- to provide a basis for comparison with similar investigations to be done in the presence of forced flow, and
- to obtain a deeper insight into the influences of impurities, step patterns and defects on the growth process.

To accomplish these tasks, we substantially redesigned our interferometric set-up. We replaced the white light source with laser illumination to increase the image contrast and to

obtain a fringe pattern that does not require readjustment as the crystal grows. In order to obtain the necessary laser power stability we used a semi-conductor laser with an output power control. In addition, the microscope was put into a styrofoam enclosure with a vinyl shroud as the front access port. The temperature in the enclosure is maintained constant within 0.1°C by means of a heater and fan operated by a temperature controller. The fan and cables connecting to the microscope setup are appropriately anchored on the laboratory to prevent vibrations from these components from reaching the interferometer, which in turn is positioned on a floating optical table. Vibrations imparted on the microscope crystal growth cell by the cooling water have been eliminated by maintaining a constant hydrostatic pressure that assures laminar flow. Through these measures we have come close to an interferometer stability of 20 mμ for several hours.

Furthermore, software packages in Microsoft C and Mathcad were developed which allow us to digitally record the displacement of the crystal faces with an accuracy of 20 mμ, which corresponds to less than three unit cell heights for lysozyme. These measurements can be simultaneously performed at up to 20 points on a crystal surface. In this way we are able to quantify minute variations in growth/dissolution morphology, from which subtle changes in the kinetics can be deduced. We are hopeful that the very early stages in the formation of 3D defects can also be monitored. The ability to detect these local variations in growth kinetics will likely be quite significant in detecting the consequences of the forced convective flow. In addition, by following the interfacial displacement at two closely (~5 μm) situated points on the crystal surface we can *directly* measure the velocity of steps propagating over the surface. So far step velocity could only be determined from the ratio of the growth rate to growth hillock slope with the assumption that the slope did not change over a wide (~0.2 mm) surface region.

2.3. Repartitioning of Precipitant

Our interest in the repartitioning between the solution and the growing crystal stems from macroscopic and microscopic considerations. Macroscopically, the repartitioning of precipitant ions during crystallization could lead to their concentration change in front of the growing interface. This could induce local change in the protein solubility, supersaturation, and is, thus, essential for comprehensive model calculations of protein crystal growth. Microscopically, we want to shed some light upon the interactions between protein molecules and precipitant ions in the mother solution, in the course of crystallization and in the crystals. Variations in the quantity of precipitant captured by the crystal under different crystallization conditions could lead to structural changes and hence influence the resulting crystal quality.

In the solution one can assume that all sites on a protein molecule's surface that are suitable for both the chemical adsorption of Cl^- and for intermolecular contacts in the crystal, are occupied by Cl^- ions. As found in colloid systems, the Na^+ ions probably form a diffuse

layer around the molecule (with associated Cl^- ions) to ensure charge neutrality. When the molecule becomes (gradually) bound onto and into the crystal, at least the chloride ions that occupy intermolecular contact sites (together with some Na^+ ions) are probably rejected at the crystal-solution interface.

Crystallization experiments were carried out at temperature T = 4 °C in test tubes containing 10 ml of solution with 2.5 % NaCl at pH = 4.5. The equilibrium concentration for lysozyme under these conditions is C_e = 2.8 mg/ml. Thus, with lysozyme concentrations between 8 and 50 mg/ml we covered a range of supersaturation ratio $\sigma = C/C_e$ from 2.8 to 17.

The quantities of lysozyme and of the precipitant ions were determined in the initial solution, the supernatant and in the crystals; for the latter the crystals were dissolved in deionized water. The lysozyme contents were measured by UV spectrophotometry. Na^+ concentrations were determined by atomic absorption spectroscopy. Prior to the measurement of $[Cl^-]$ by ion selective potentiometry, lysozyme was separated from the sample by ultrafiltration. In all runs the mass balance for lysozyme and sodium checked out within 5%.

From these measurements, the numbers of Na^+ and Cl^- ions per lysozyme molecule in the crystals, in the supernatant and in the initial solution were determined. The effective segregation coefficient k was calculated as

$$k = \frac{(N_{ion}/N_{lysozyme})^{crystal}}{(N_{ion}/N_{lysozyme})^{solution}} \quad .$$

We carried out three types of experiments.

(a) In the first type, various initial supersaturations were used. Crystals were separated from the supernatant after about a week. Accordingly, depending on the initial supersaturation, from 10 to 60 % of the protein crystallized in the different test tubes. Thus some of the crystals grew under significantly decreasing supersaturation conditions.

(b) In the second type, the supersaturation was again different in different test tubes. However, to obtain crystals that grew at essentially constant supersaturations, the crystals were separated from the solutions after ~5% had crystallized. This meant crystallization times between a few hours for the lysozyme concentration of 40 mg/ml to 10 days for 10 mg/ml.

(c) In the third type, we had a constant lysozyme concentration of 40 mg/ml, i.e. the highest concentration used in the type (b) experiments. In order to observe a possible time dependence of the partitioning we removed the crystals at different times: from 6 hours to 8 days, with 3 - 85 % of the protein crystallized, respectively.

Fig. 1 shows for three experiments of type (a) the dependence of the relative quantity of the ions captured in the crystals on the initial supersaturation. As one would expect from charge neutrality at pH = 4.5, the quantities of Na^+ are always somewhat less than those of Cl^-.

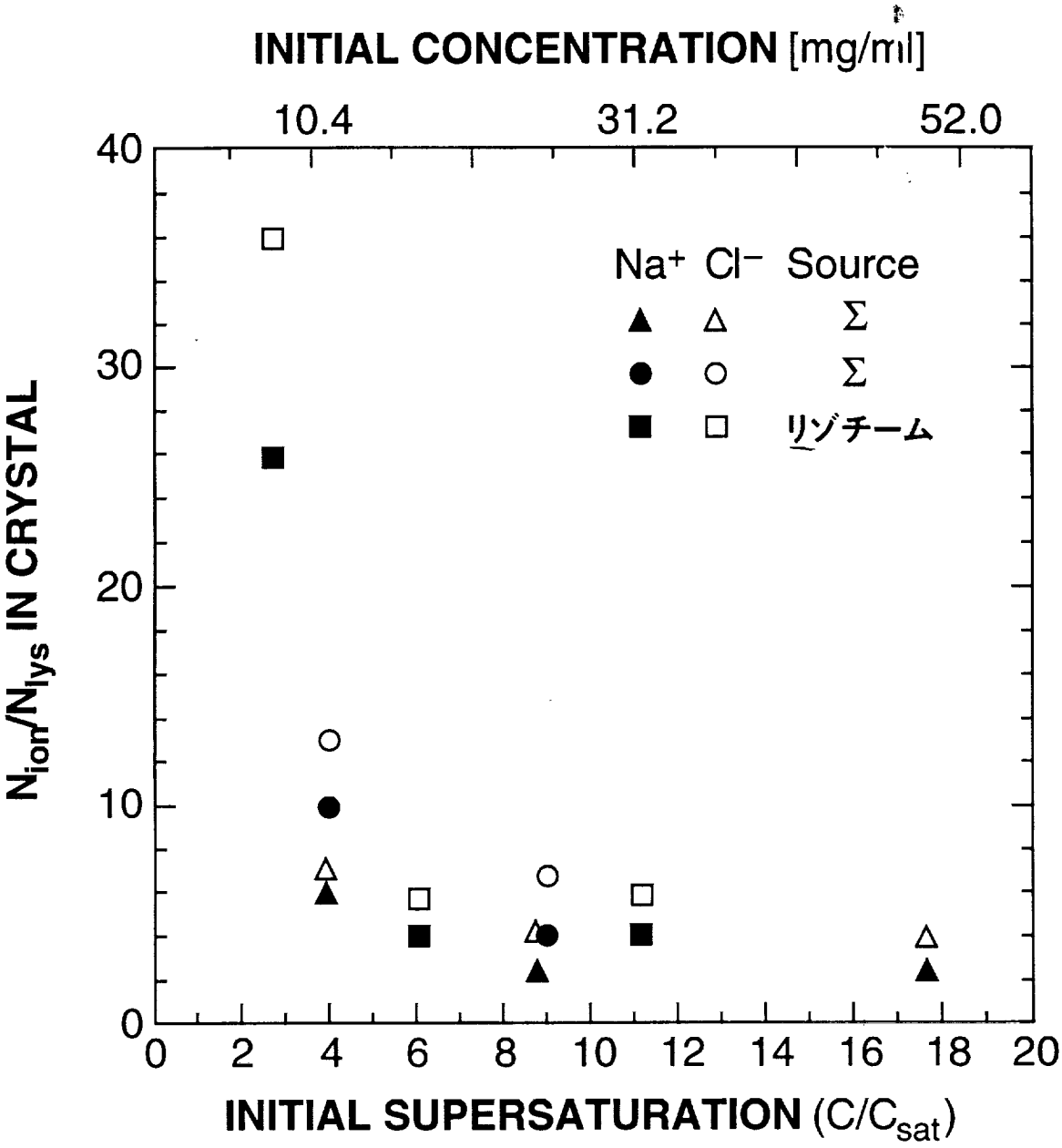
INITIAL CONCENTRATION [mg/ml]
10.4
31.2
52.0
40
30
20
10
0
Na+ Cl− Source
Σ
Σ
リゾチーム
N_{ion}/N_{lys} IN CRYSTAL
0 2 4 6 8 10 12 14 16 18 20
INITIAL SUPERSATURATION (C/C_{sat})

FIG. 1

However, quite unexpectedly, the amount of incorporated ions decreases with increasing initial supersaturation and, hence, increasing growth rate. Such a behavior can, for instance, be the result of an interaction of the ions with some other component (impurity) with growth rate-dependent segregation. The presence of, likely, large molecule impurities in lysozyme solutions was recently evidenced by analytical measurements and crystal growth kinetics studies. To check this hypothesis, we carried out experiments with lysozyme from different sources: 3x crystallized from Sigma and 6x crystallized from Seikagaku, Japan. The results (fig. 1) do not indicate any difference in the quantity of the captured salt with the different source material, thus refuting our assumption.

Another possible mechanism involves the time-dependent relocation of Cl^- ions that are adsorbed on the protein molecules. When a molecule enters the crystal, the chlorides are driven out of the intermolecular contact sites. At slow growth rates (low supersaturations) they have time to relocate on the protein molecule surface. The typical times of such reactions, of the order of 1 ms, are comparable to the times between protein molecules joining the crystal. At higher growth rates (supersaturations) molecules impinge on potential growth sites with higher frequency and the Cl^- ions have insufficient time to bind to another suitable place so they are left out of the crystal.

The main assumption in the above hypothetical mechanism is the time-dependent relocation of the Cl- ions. To test this hypothesis we have planned experiments with ions that would be still slower, for example Br^-. If, whith NaBr as a precipitant, the dependence corresponding to fig. 1 is shifted to the right, this would support the above model.

As depicted in fig. 2, the experiments of the second type show the same trend of decreasing number of sodium and chloride ions with increasing supersaturation. Rather surprisingly, however, the numbers are several times larger then in the previous case. This could be a surface effect. The smaller crystals resulting in type (b) experiments have a much larger surface-to-bulk-ratio than the the type (a) ones. Remnants of the solution on the crystal surface after separation, or an adsorption layer rich in precipitant ions could bias our measurements. To exclude such interference, the crystals in another type (b) experiment were rinsed with 1 ml of 4 °C deionized water. Observation under the microscope revealed that the crystals were slightly etched. As fig. 2 shows, this washing did not change the apparent Cl^- and Na^+ intake. Hence, we conclude that the higher values are not due to a surface effect.

The effective segregation coefficients obtained from the data in fig. 2 are plotted with corresponding symbols in fig. 3. Within the rather large error limits of these "four component data", there seems to be little dependence of k on supersaturation .

Although experiments of type (a) and (b) resulted in the same trends with respect to supersaturation, they yielded largely differing relative quantities of incorporated ions. To further

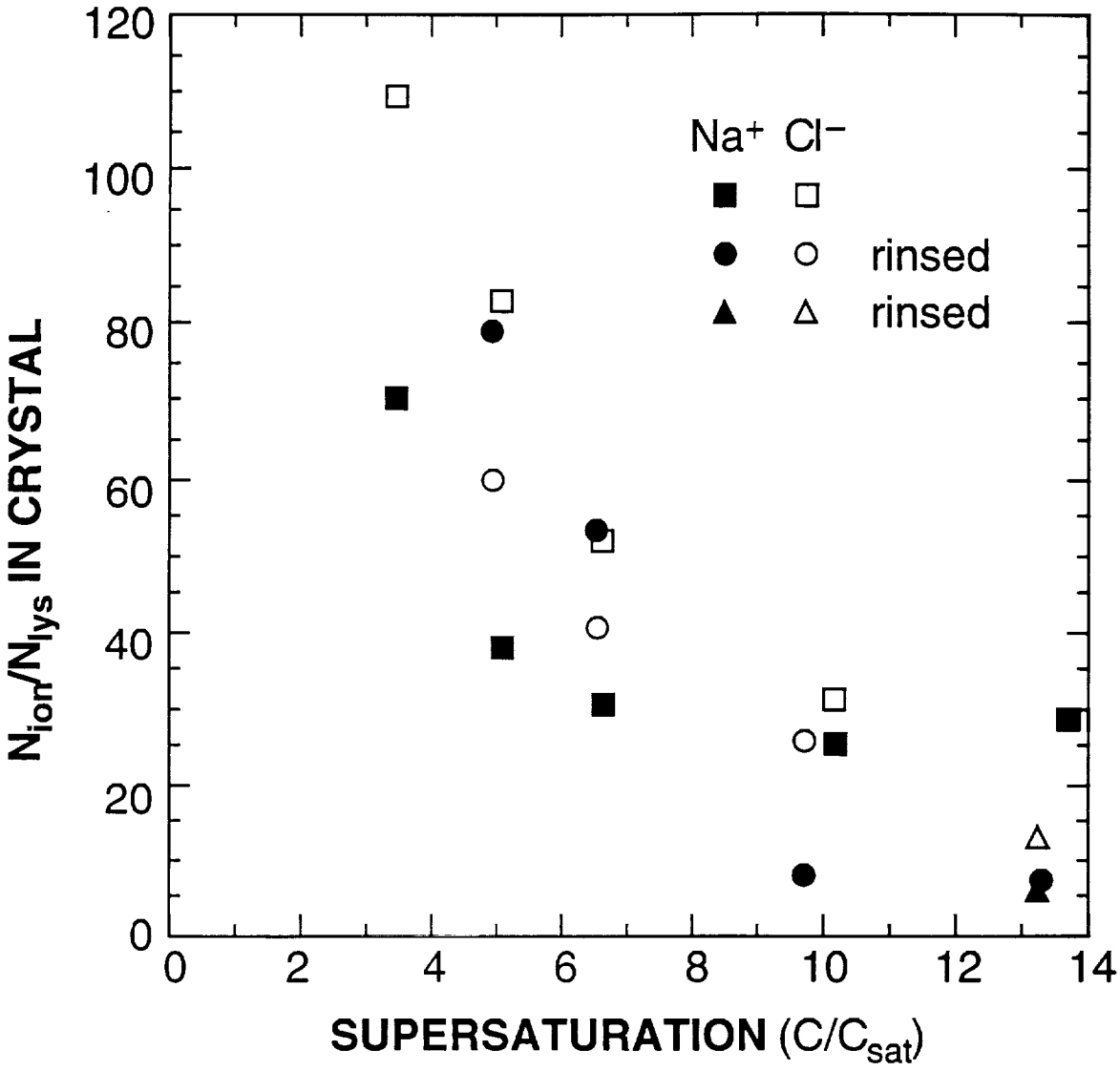
120
100
80
60
40
20
0
0
2
4
6
8
10
12
14
N_{ion}/N_{lys} IN CRYSTAL
SUPERSATURATION (C/C_{sat})
Na^+ Cl^-
rinsed
rinsed

FIG. 2

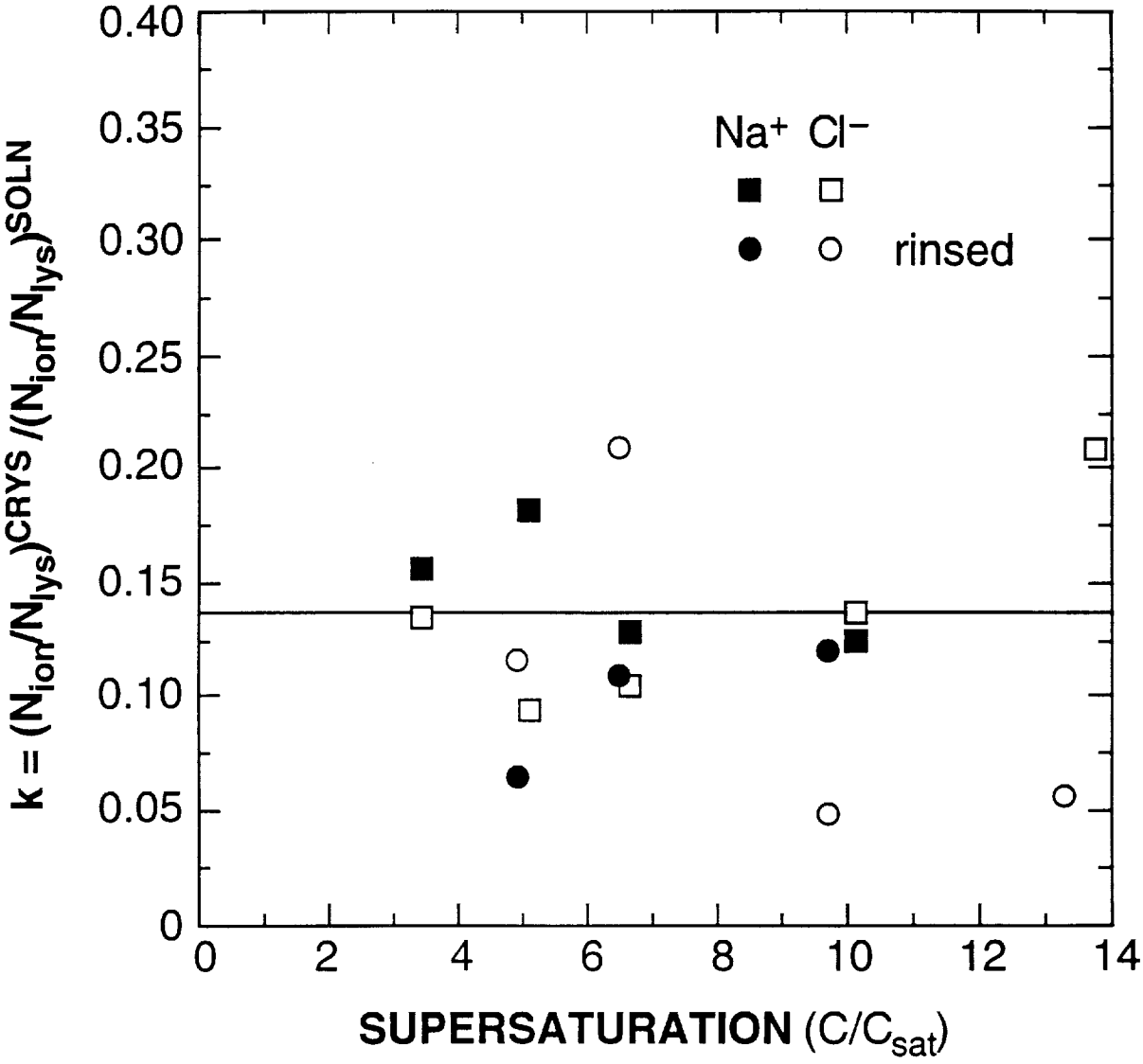
0.40
0.35
0.30
0.25
0.20
0.15
0.10
0.05
0
0
2
4
6
8
10
12
14
Na+ Cl−
rinsed
k = (Nion/Nlys)CRYS /(Nion/Nlys)SOLN
SUPERSATURATION (C/Csat)

FIG. 3

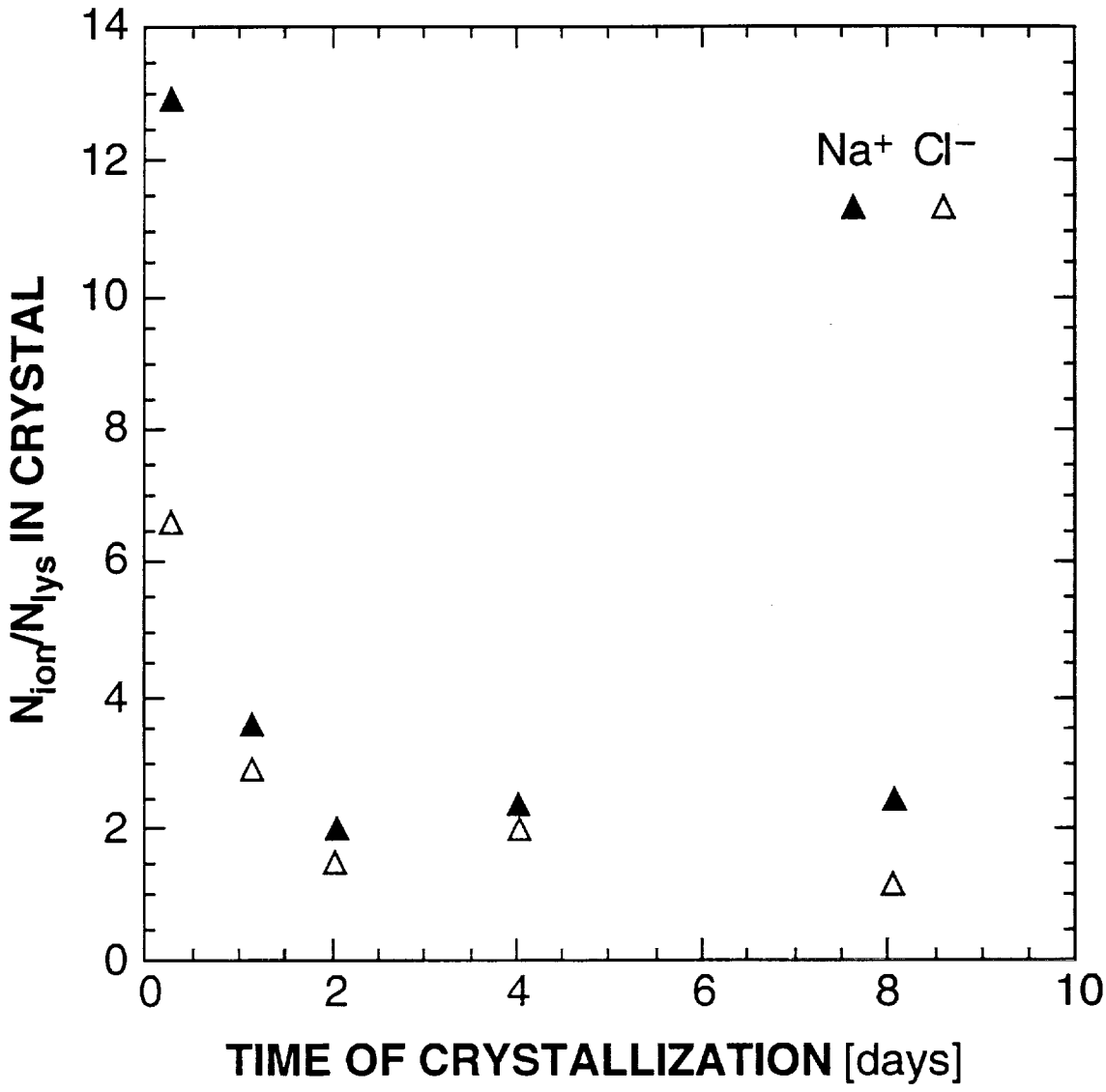
14
12
10
8
6
4
2
0
0
2
4
6
8
10
Na+ Cl−
N_ion/N_lys IN CRYSTAL
TIME OF CRYSTALLIZATION [days]

FIG. 4

investigate this disparity, we followed the dependence of the captured ion quantities on the crystallization time at constant supersaturation $\sigma = 13.2$. The results are plotted in fig. 4. For the shortest crystallization time, the same results were obtained as in the (b) series at $\sigma = 13.2$. For the longest crystallization time ($t \approx 8$ days) the results roughly coincide with the values that one obtaines from an interpolation of the results to this supersaturation in series (a). The Na^+ concentrations found throughout this series are higher than the Cl^- concentrations, in contrast to the results of the type (a) and (b) experiments. But even more interestingly, the overall trend is that the quantity of the captured ions decreases with the time the crystals are in contact with the solution. This behavior is not understood at all. An important consequence of this possible "out-diffusion" process could be a change in the crystallographic structure of the protein crystal with time of contact with the solution. For more definitive conclusions we need to confirm the effect by an experiment at a different supersaturation, then we will probably change the source material to investigate possible impurity influence.

2.3. Numerical Modelling of Diffusive-Convective Transport

In order to investigate the mass transport process and how convection affects protein crystal growth, a realistic model is very useful. We have developed a time-dependent, two-dimensional model of convective-diffusive transport in protein crystal growth that includes finite rate kinetics. This model can provide information about the evolution of (1) concentration distributions of the various species present in the nutrient solution, (2) crystal surface concentrations and growth rates and (3) convective velocity fields. The interplay between transport and growth morphology dependent kinetics will be included in the future.

Model

The simplified two-dimensional geometry assumed for this model is shown in fig.1. The geometry for this study was based on an actual experiment set-up used in our laboratory for growth morphology studies on protein crystals. We simplified the actual protein crystal growth cell to two dimensions and put the crystal seed at the center of the cell bottom. The growth cell is 6 mm × 1 mm, crystal size is 0.6 mm × 0.4 mm. Because of the low face growth rates of protein crystals, it is reasonable to assume that the crystal shape and size remain unchanged to avoid a moving boundary problem. In addition, we assume the cell is maintained isothermally.

The transport of mass, momentum, and species is governed by the following equations (in the Boussinesq approximation and in dimensionless form),

Continuity $\quad \nabla \cdot \mathbf{V} = 0;$

Momentum $\quad \dfrac{\partial \mathbf{V}}{\partial t} + \mathbf{V} \cdot \nabla \mathbf{V} = -\nabla p + \nabla^2 \mathbf{V} + \dfrac{Ra}{Sc} \rho_1 \mathbf{g};$

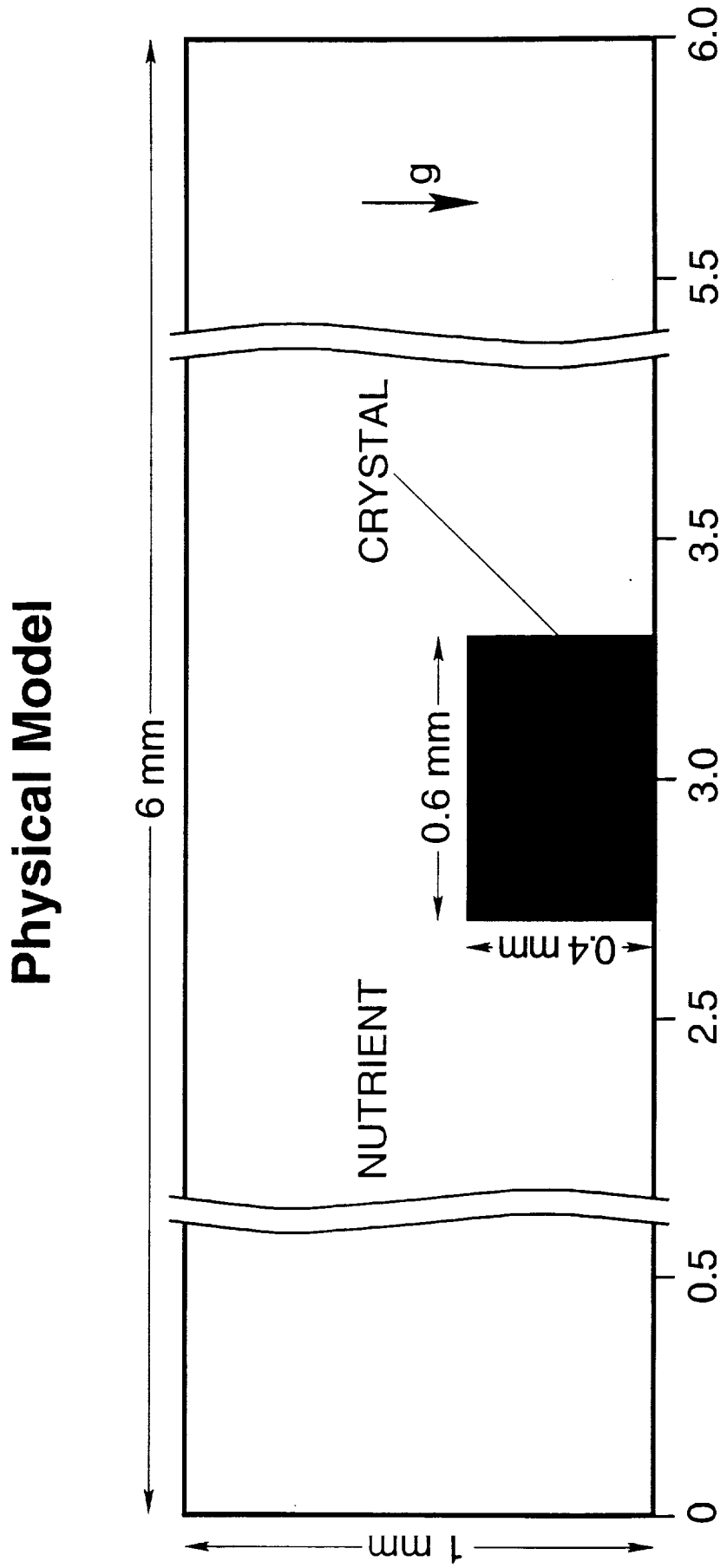

Simplified model geometry employed for simulation of protein crystal growth

FIG. 1

Species $$\frac{\partial \rho_j}{\partial t} + \mathbf{V}\cdot \nabla \rho_j = \frac{1}{Sc}\nabla^2 \rho_j \quad (j = 1, \text{protein};\ 2, \text{salt}).$$

Here, $\mathbf{V}$, p, ρ_j are the dimensionless velocity, pressure, and species mass densities in the solution, respectively; while $\mathbf{g}$ is the dimensionless gravitational acceleration. The characteristic parameters used for non-dimensionalization are the crystal width ℓ for length, ℓ^2/ν for time (where ν is the kinematic viscosity) and the initial protein mass concentration ρ_1^0. The dimensionless parameters of solutal Rayleigh number and Schmidt number are,

$$Ra = \ell^3 g_0 \beta_c \rho_1^0 / D\nu,$$

$$Sc = \nu / D,$$

with g_0 the terrestrial gravitational acceleration (9.8 ms^{-2}), D the solute (protein) diffusivity, β_c the coefficient of solutal expansion.

The boundary conditions at the cell wall are those of non-slip and solute impermeability in the form of

$$\mathbf{V} = 0,$$

$$\nabla C_j \cdot \mathbf{n} = 0.$$

At the interface, using mass balance and Fick's Law, the normal solutal velocity has the form of

$$\mathbf{V}\cdot\mathbf{n} = \frac{\rho^c}{\rho^s}\mathbf{V}^f,$$

where ρ^c and ρ^s are, respectively, the total density of the crystal and solution,. $\mathbf{V}^f$ is the crystal face growth rate. The tangential velocity on the interface is zero, $\mathbf{V}\times\mathbf{n} = 0$.

The choice of face a growth rate condition for the crystal, i.e., a realistic connection between mass transport and interface kinetics, is much more difficult. Based on their experimental measurements, Pusey and Naumann suggested a quadratic dependence of the growth rate on supersaturation for the lysozyme (110) face. Other authors suggested different relationships. However, all these rate expressions are based on bulk supersaturation measurements and no data are available on the growth rate as a function of *interfacial* supersaturation. Additionally, too little is known about the protein crystal growth mechanism itself to theoretically predict a rate expression.

In general, the driving force for crystal growth is given by the chemical potential difference of the solute in the solution next to the interface and in the crystal, $\mu^i - \mu^c$. With the ideal solution assumption, setting all activity coefficients to unity, and assuming low supersaturations, this difference can be written as

$$\mu^i - \mu^c \approx kT \ln C^i / C^{eq} \approx kT\,(C^i - C^{eq}) / C^{eq}$$

where C^i is the interfacial protein molar concentration and C^{eq} is the molar solubility.

Motivated by this formulation and approximating the result of the most recent growth rate kinetics studies with lysozyme in our laboratory, a linear relation between face growth rate and interfacial supersaturation was used in this study. We can get the interface concentration boundary condition by using mass balance and Fick's law, in the form of

$$\text{growth rate} = k\,[(\rho_1^i - \rho^{eq})/\rho^{eq} - \sigma_0] = -D\,\nabla\rho_1 \cdot \mathbf{n} / (\rho_1^c - \rho_1^i \rho^c / \rho^s)$$

where the kinetic coefficient $k = 7.9 \times 10^{-10}$ m/s and $\sigma_0 = 3.0$ are experimental constants, ρ_1^i the calculated interfacial protein mass concentration, ρ^{eq} the protein mass solubility, ρ_1^c the protein mass concentration in the crystal. A Newtonian iterative method is employed to solve this non-linear equation. At each time step, this equation is solved to get the interfacial concentration, which, in turn, modifies the face grwoth rate.

As initial conditions we assumed the fluid at rest and uniform concentration of lysozyme ρ_1^0 everywhere,

$$\mathbf{V} = 0 \text{ and } \rho_1 = \rho_1^0 \quad \text{at } t = 0.$$

Numerical Scheme

We employed the finite volume approach to discretize the domain equation. For the temporal domain we used the implicit Euler scheme; in the spatial domain, the central differencing scheme for diffusion terms and the upwind scheme for convection terms.

In solving for incompressible fluid flows, there is always the problem of how to couple the velocity and pressure because of the weak relation between pressure and density. To circumvent this problem, we have used the PISO (Pressure Implicit with Splitting of Operators.) method, which is non-iterative and is more accurate than the SIMPLE or SIMPLER method widely used in the 1980s. For solving the discretized equations, we employed the conjugate-gradient-squared method to enhance the matrix solver efficiency.

It is well known that non-staggered grid systems can produce undesirable "checker-board" (oscillatory) phenomena in the pressure field due to the decoupling between velocity and pressure. Hence,we used a coordinate system with a non-staggered grid arrangement, i.e., all variables are specified at the same grid points. In addition, we use pressure damping to modify the finite volume face velocity at each correct step to avoid the "checker-board" of the pressure field.

We are particularly interested in the concentration distributions around the protein crystal. Due to the low diffusivities of protein solutions, we can expect that most of the concentration change occurs in a narrow layer at the growing crystal. Hence, we have used a finer grid near the crystal than in the bulk solution. Figure- 2 shows the non-uniform 19×45 mesh employed in the simulations, which was generated according to the power law.

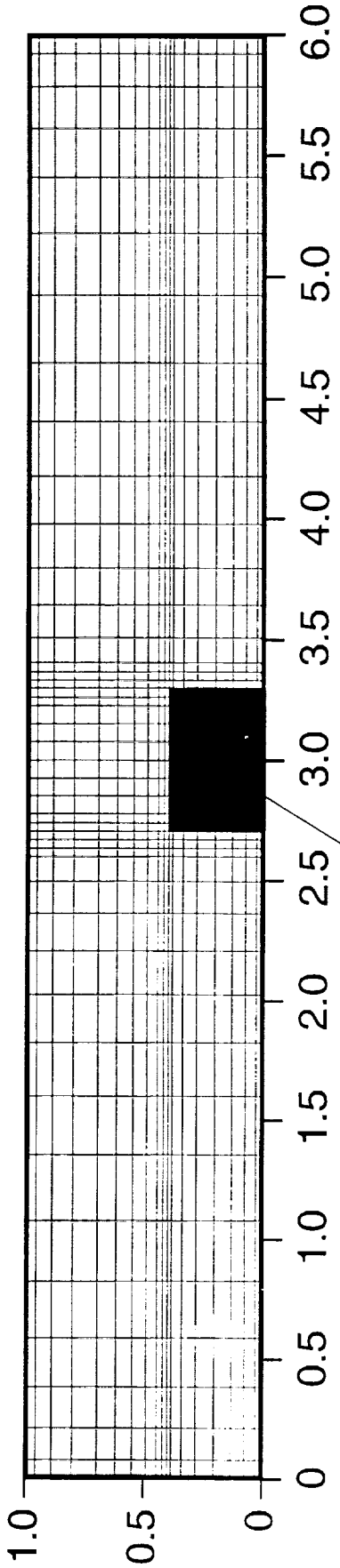

The 45 × 19 mesh used in simulations.

FIG. 2

Results

This investigation is still in its initial stages. Salt segregation is not well understood at this point. Some experiments showed that in lysozyme crystals each lysozyme molecule is associated with about 10 Cl^-. This corresponds to a mass concentration of ρ_2=33.5 mg/ml. If we assume that in the solution each lysozyme molecule is associated with 18 Cl^-, there will be 8 Cl^- released at the interface into the solution on incorporation of a lysozyme molecule into the crystal. For simplicity, we do not distinguish between Na^+ and Cl^- and consider the ions only in units of salt molecules. This is schematically dipicted in the following figure.

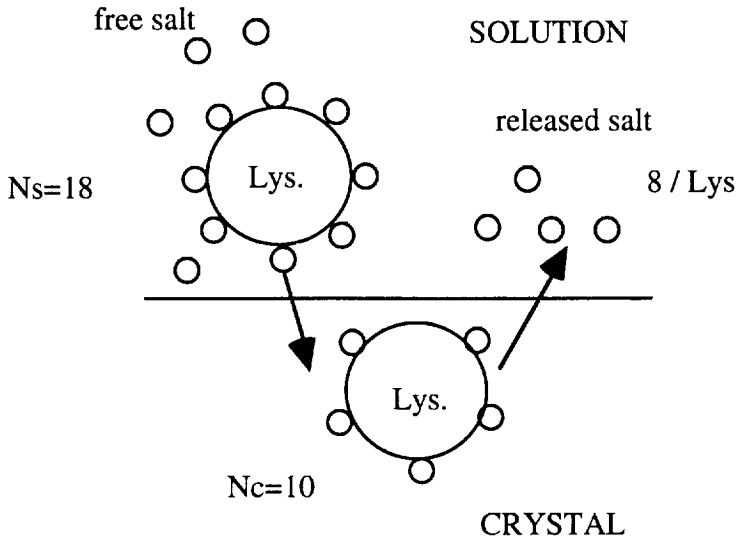

Salt Segregation at Crystal Interface

From the mass balance for salt at the interface , we can get the salt interface boundary condition

$$(N_2^s - N_2^c) \frac{M_2}{M_1} \rho_1^c \mathbf{V}^f = -D_2 \nabla \rho_2 \cdot \mathbf{n} \ ,$$

where N^s and N^c are the numbers of associated salt molecules per lysozyme in the solution and crystal, respectively, and M_1 and M_2 are the molar weight of salt and lysozyme. Using this condition and M_2 / M_1=58 / 14600 = 3.97×10^{-3}, D_{salt}=1.6×10^{-5} cm^2s^{-1}, ρ_1^c = 838.44 mg/ml and $\mathbf{V}^f = 10^{-6}$cm/s, we can estimate the salt gradient at the interface to be

$$\nabla \rho_2 \cdot \mathbf{n} = 2.082 \times 10^5 \text{ (Ns - Nc) } V_F = 0.2 \text{ } (N^s - N^c) \text{ mg/(ml mm)}.$$

This result suggests that the salt gradient at the interface is likely to be small as compared to the salt concentration in the bulk scaled with the cell height of 1 mm. Consequently, the salt distribution will be rather uniform throughout the solution, and salt will contribute much less

than the protein to solutal convection. Hence, in our preliminary calculations we have neglected salt segregation at the interface.

The following results were obtained for solutions with lysozyme concentration 5% w/v; 2.5% w/v salt; pH = 4.5 at temperature 12°C. For these conditions, the solubility of lysozyme $\rho_1^{eq} = 3.1$ mg/ml.

Figure 3 shows the solutal convective velocity field after one hour of crystal growth. The classic convective flow pattern for solution growth can be seen with a rising plume above the crystal. When the crystal begins to grow, the solutal concentration around the crystal seed decreases because of the incorporation of protein. Gravity causes the light solution to move upwards. The maximum value of convective velocity obtained at that time is approximately 10 μm/s, which is much higher than the diffusive velocity for lysozyme of $D/\ell = 0.2$ μm/s . This result shows that even in the small growth cells typically employed for protein crystal growth, solutal convection can become so large that it dominates the transport of solute from the bulk solution to the crystal.

The difference that solutal convection can make for the transport can be seen even more clearly from a comparison of the protein concentration distributions for purely diffusive transport (g = 0, fig.4) and for transport with solutal convection (g=1, fig.5). With convection, the lysozyme concentration in the nutrient is more uniform. This leads to higher growth rates and as shown in fig.6, a slower decrease of crystal face growth rate with growth time. With purely diffusive transport significant concentration gradients in the solution and growth rate non-uniformities persist.

Our simulations reveal that the protein concentration at the interface and, correspondingly, the growth rate, is not uniform irrespective of the prevailing transport mode. This is further illustrated with the detailed growth rate distributions for the top face, fig. 7, and side faces, fig. 8, for both 1g and 0g. This comparison indicates that *from a mere transport point of view,* convection can be beneficial since it caused a higher face growth rates, and on some faces, a more uniform growth rate distribution. From fig.3, we see that the maximum convective velocity occurs around the crystal corners which causes the interfacial concentration to be highest at these locations. The corresponding higher growth rate at crystal corners is consistent with experimental observations in our laboratory. In order to draw more detailed conclusions about convection effects on protein crystal growth, more detailed accounts of interfacial kinetics mechanisms must be incorporated into the model. This and detailed considerations of the role of the precipitant will be included in future work.

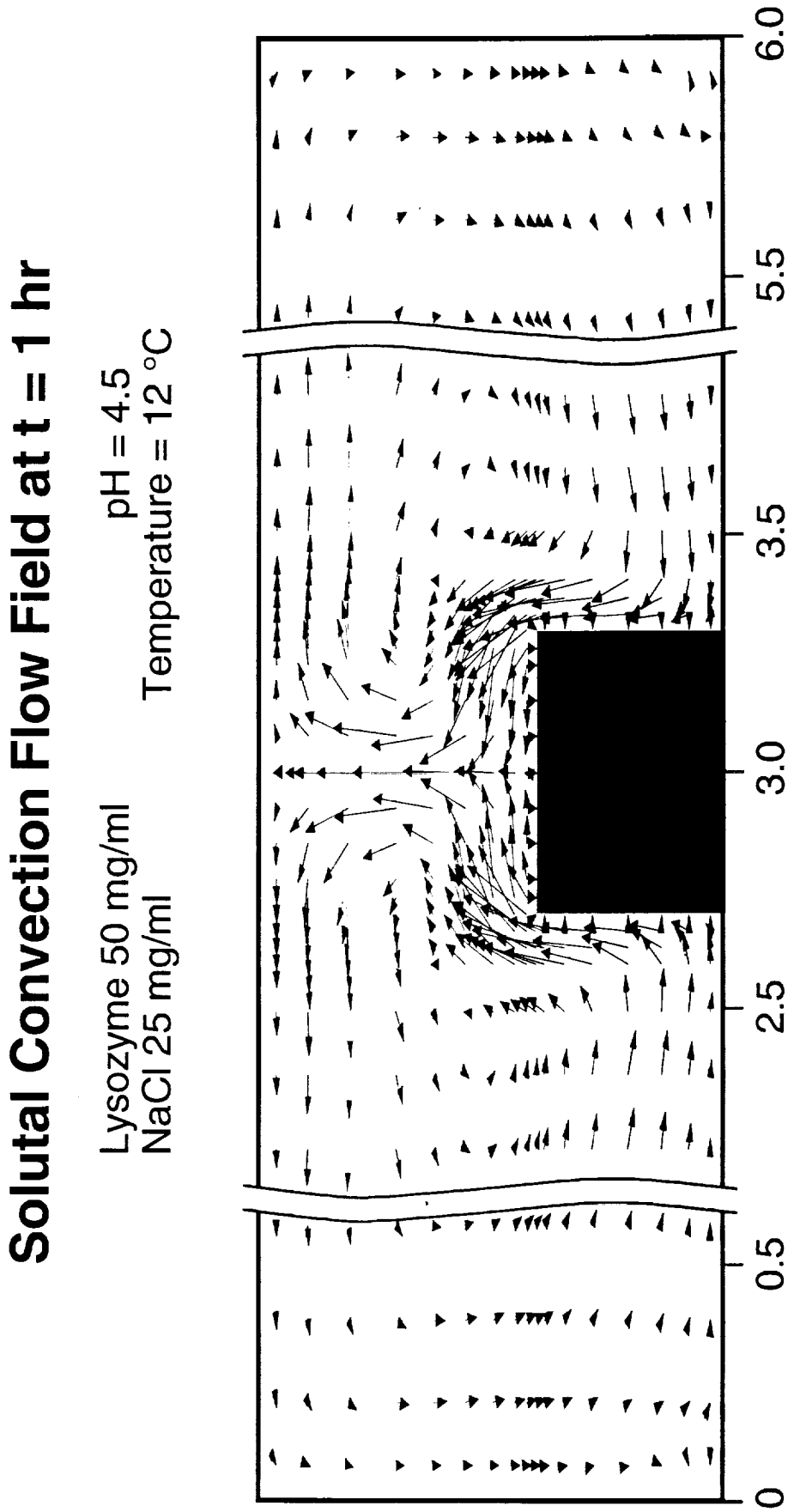

Velocity field at t = 1 hr. The maximum velocity is 8.62×10^{-4} cm/s near the top corners of the crystal.

FIG. 3

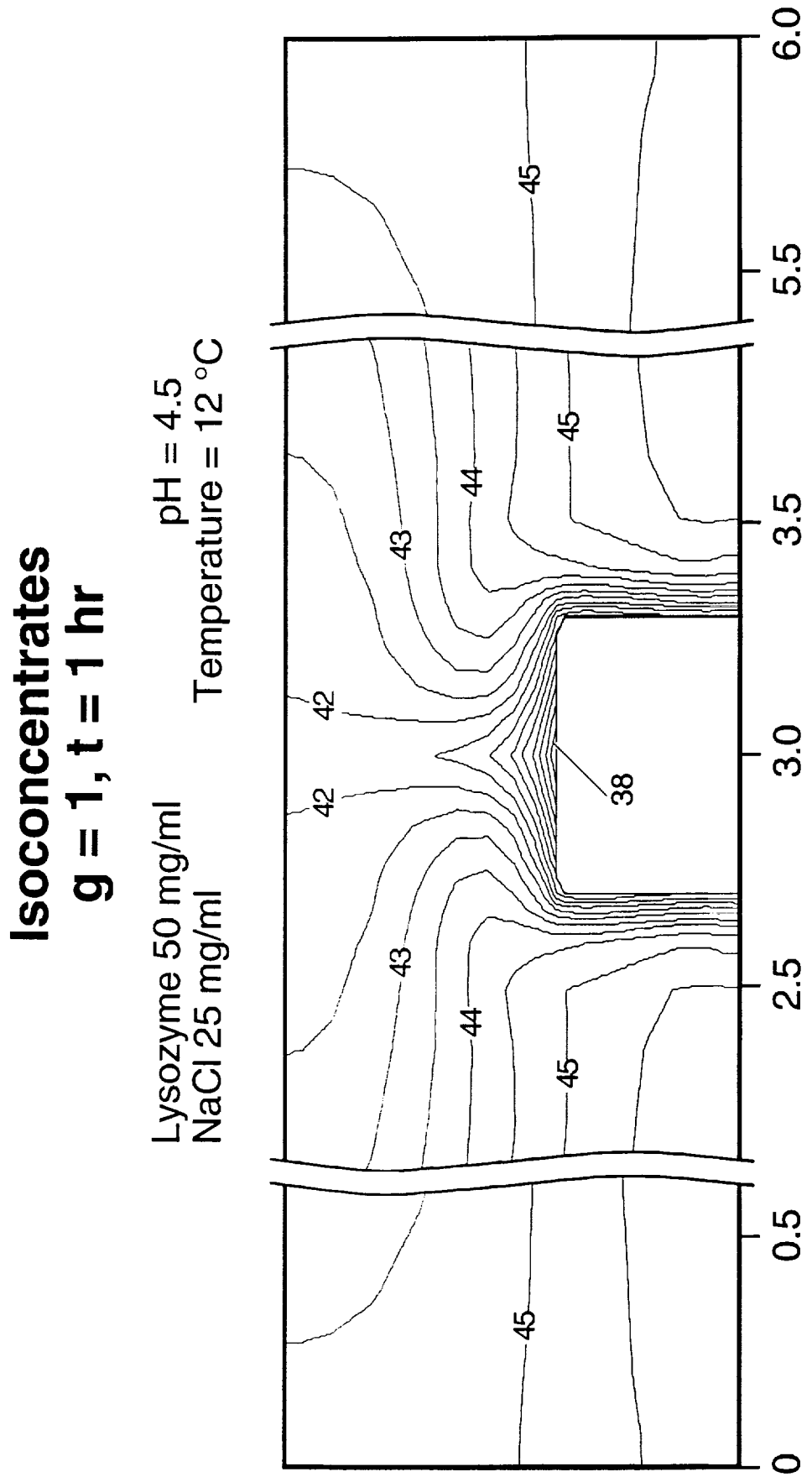
Isoconcentrates
g = 1, t = 1 hr
Lysozyme 50 mg/ml
NaCl 25 mg/ml
pH = 4.5
Temperature = 12 °C
0
0.5
2.5
3.0
3.5
5.5
6.0
45
44
43
42
38

FIG. 4

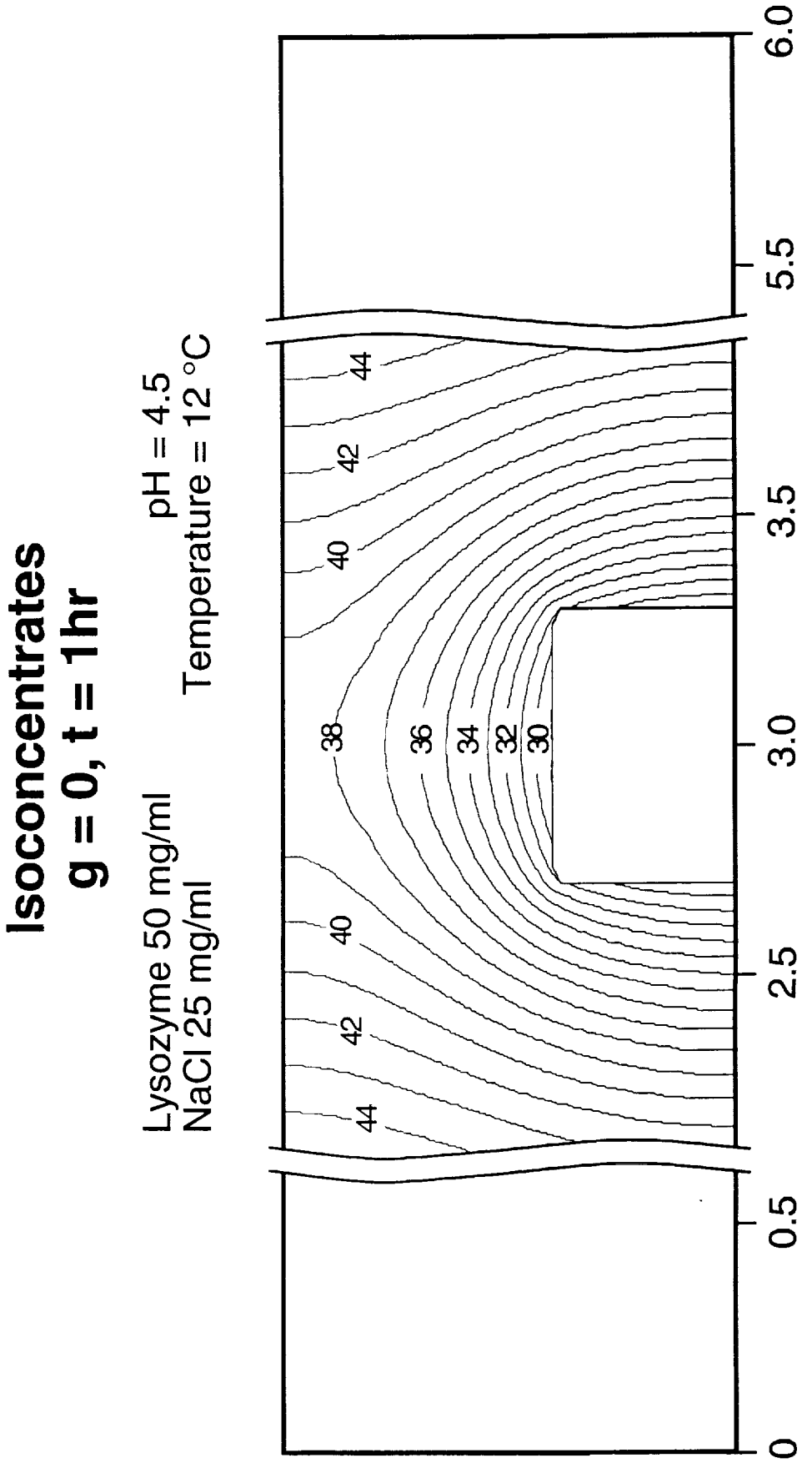
Isoconcentrates
g = 0, t = 1hr
Lysozyme 50 mg/ml
NaCl 25 mg/ml
pH = 4.5
Temperature = 12 °C
44
42
40
38
36
34
32
30
40
42
44
0
0.5
2.5
3.0
3.5
5.5
6.0

FIG. 5

Growth Rates vs. Time at Selected Positions

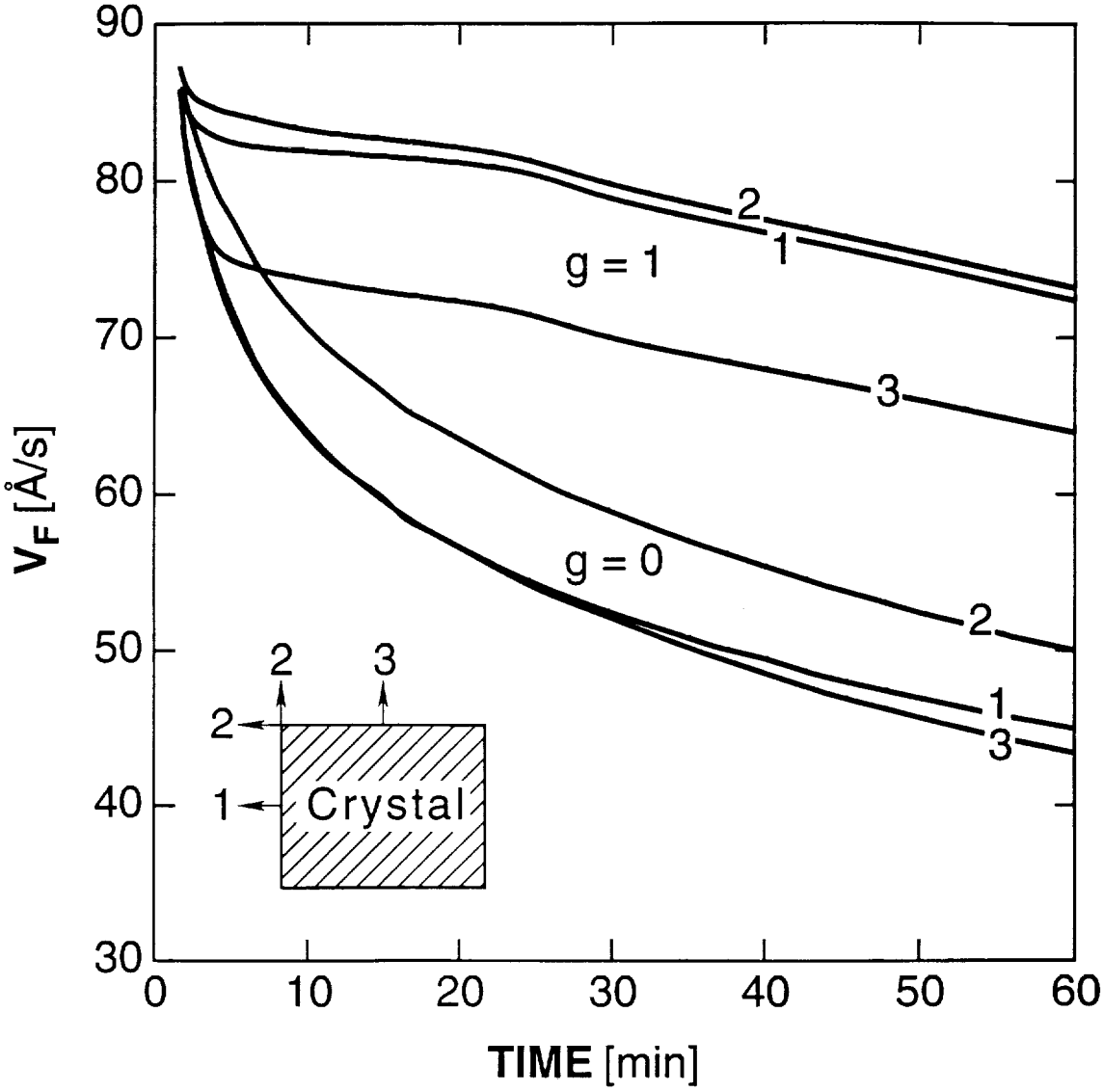

FIG. 6

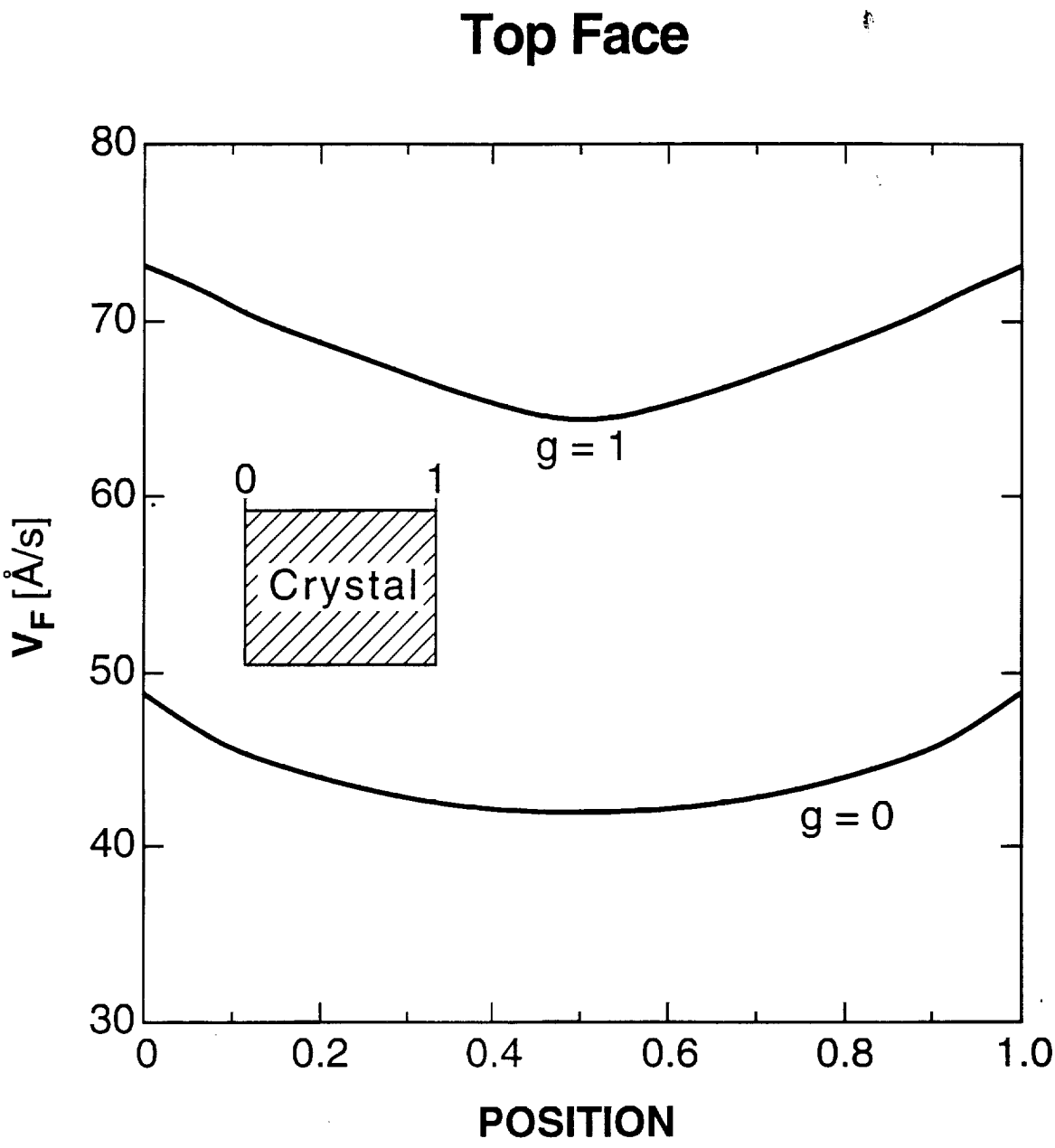
Top Face
80
70
60
50
40
30
V_F [Å/s]
g = 1
g = 0
0
1
Crystal
0
0.2
0.4
0.6
0.8
1.0
POSITION

FIG. 7

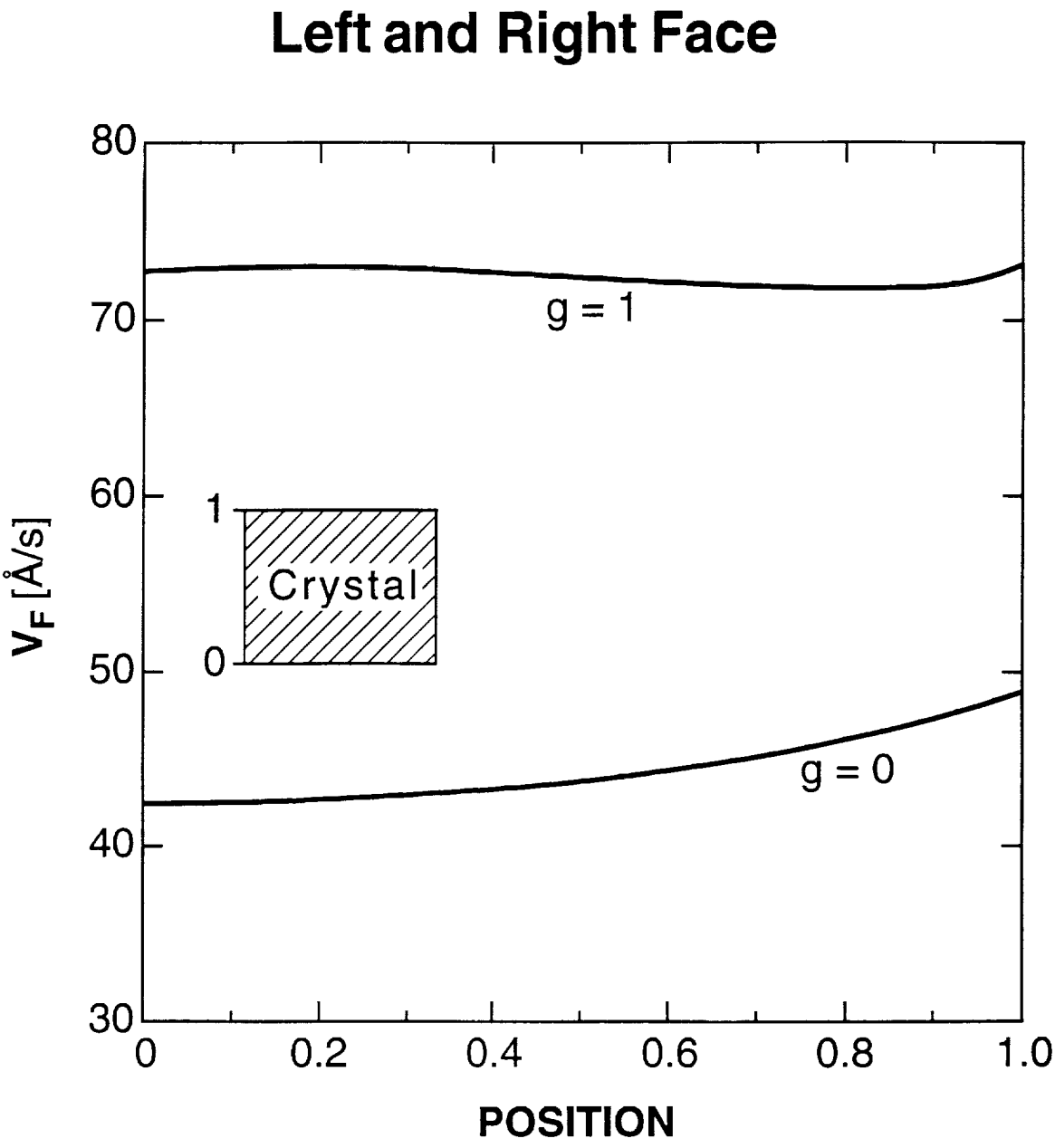
Left and Right Face
80
70
60
50
40
30
V_F [Å/s]
g = 1
g = 0
1
Crystal
0
0
0.2
0.4
0.6
0.8
1.0
POSITION

FIG. 8

2.4. Kinematic Viscosity Measurements

The viscosity of lysozyme solutions was monitored over time under conditions which are known to lead to crystallization. Supersaturated hen egg-white lysozyme solutions with various concentrations of protein and sodium chloride as the precipitating agent (see Table below) and 50 mM pH=4.5 acetate buffer were used. A Cannon-Fenske routine viscometer was used to determine the kinematic viscosities based on the efflux time of the solutions through the capillary of the viscometer. The viscometer constant provided by the manufacturer was confirmed through calibration runs with deionized water. The viscometer was temperature controlled to ±0.2 C° using a water bath. Changes in the kinematic viscosity of aqueous solutions by 1% could be detected. The solutions were kept in the sealed viscometer and the efflux time was measured every few hours until crystals were detected by laser illumination in the solution. The 42 mg/ml lysozyme sample was aged outside of the viscometer. Samples from this solution were transfered to the viscometer with a 0.2 μm pore size filter syringe right after crystallization was detected, and when a considerable fraction of the protein had crystallized.

Lysozyme Conc. (mg/ml)	NaCl Conc. (% m/v)	Temperature (C°)	Kinematic Viscosity vs. Time (cS)
50	2.5	25	1.22 through 50 hrs to crystallization
55	2.9	15	1.52 through 3 hrs to crystallization
65	2.9	15	1.62 through 2 hrs to crystallization
27	4.0	25	1.03 through 75 hrs to crystallization
75	2.0	25	1.25 through 60 hrs to crystallization
48	2.9	20	1.29 for 23 hrs to 1.43 after 30 hrs
48	2.9	20	1.28 through 50 hrs to crystallization
48	2.9	20	1.29 through 96 hrs to crystallization
48	2.9	20	1.28 through 30 hrs to crystallization
42	2.9	20	1.21 through the 50 hrs to crystals and 1.13 after some crystallization

With the exception of one of the 48 mg/ml lysozyme and 2.9% NaCl sample that likely crystallized in the capillary of the viscometer, thereby obstructing the flow and increasing the efflux time, none of the solutions studied showed a change in kinematic viscosity as the solutions aged before crystallization. Only the 42 mg/ml lysozyme sample showed a change in kinematic viscosity κ. Noting that κ is the viscosity divided by density, this change cannot be explained in

terms of the density decrease that the solution undergoes upon crystallization of the protein. This result requires further investigation

2.5 Light Scattering

Workshop on Characterization of Liquids Using Light Scattering

On July 1-2, 1993, we conducted a small workshop on laser light scattering and application to the characterization of aggregates and nuclei in protein solutions. Theoretical and state-of-the-art experimental aspects were covered; see the schedule and list of speakers that is appended to this report. Attendees included UAH, UAB and MSFC personnel.

Light Scattering Studies

The first step in crystallizing proteins from aqueous solutions is to establish conditions under which the solution will produce crystalline aggregates (craggs) instead of amorphous precipitate (praggs). Our recent work has focused on various aspects of the analysis necessary to identify these conditions, based on static and dynamic light scattering results.

The quantity measured in dynamic light scattering experiments is the intensity correlation function

$$G_2(\tau) \equiv \int_0^\infty dt\, I(t)\, I(t+\tau)\,. \tag{1}$$

However, the function that is commonly used for extracting, e.g., particle size distributions from these measurements is the field correlation function

$$G_1(\tau) \equiv \int_0^\infty dt\, E(t)\, E(t+\tau)\,. \tag{2}$$

For the gaussian scattering fields from ergodic protein solutions, the intensity and field correlation function are related by the Siegert relation

$$g_2(\tau) = |g_1(\tau)|^2 - 1,$$

where $g_1(\tau) = G_1(\tau) / \langle I \rangle$, $g_2(\tau) = G_2(\tau)/\langle I \rangle^2$ and $\langle I \rangle$ is the mean intensity. The simplest case of a monodisperse collection of non-interacting spherical Rayleigh scatterers leads to the following form for $G_2(\tau)$ and $g_1(\tau)$

$$G_2(\tau) = \langle I \rangle^2 [1 + \beta \exp(-2Dq^2\tau)] \tag{3}$$

$$g_1(\tau) = \sqrt{\beta}\, \exp(-Dq^2\tau) \tag{4}$$

where β relates to the spatial coherence of the signal, D is the diffusion constant and

$q = 4\pi n/\lambda \sin(\theta/2)$ is the magnitude of the scattering vector at some scattering angle θ.

Converting $G_2(\tau)$ to $g_1(\tau)$ requires subtracting the background term. This creates the following two problems: First, the background term $\langle I \rangle^2$ is very sensitive to residual dust in the solution and the inherent noise on the signal at low to moderate count rates. For a meaningful conversion, however, its value needs to be known to better than 1% accuracy. Furthermore, it is necessary to sample the correlation function over delay times spanning several decay times $\tau_q = 1/Dq^2$. For a correlator with linearly spaced delay channels most data points are therefore close to the background value and their mutual difference quickly approaches the size of the intrinsic noise on the data.

To explore these issues, we prepared aqueous solutions of polystyrene spheres of known size (63±3 nm) as test sample and collected correlation functions at 90° scattering angle. We then performed a three-parameter nonlinear least-squares fit (NLLS) to $G_2(\tau)$, a two-parameter NLLS fit to $g_1(\tau)$, and a two-parameter linear least-squares fit (LLS) to the logarithm of $g_1(\tau)$. The fit to the latter is the basis for most correlator programs in extracting D or any subsequent cumulant analysis.

We find that the values of D obtained from these various fitting methods can vary as much as 15%, predominantly due to the progressive error accumulation transforming $G_2(\tau)$ over $g_1(\tau)$ into $\ln[g_1(\tau)]$. This emphasizes, that $G_2(\tau)$ presents the best starting point when determining D from samples with tight distributions of particle size. The required nonlinear fits can - by now - be efficiently performed on personal computers.

As aggregation occurs in the samples, some type of particle size distribution information needs to be deduced from our kinetic studies of the aggregation process. The problem is, that there are only few programs to obtain size- or mass distributions from $G_2(\tau)$ directly, and they are in an experimental stage. The usual starting point is to invert the relation

$$g_1(\tau) = \int dm\, m\, \rho(m)\, S(k,m) \exp(-D(m)q^2 t) \qquad (5)$$

where $\rho(m)\, dm$ is the molecular weight distribution function, S(k,m) is the particle structure factor and D(m) is the molecular weight adjusted diffusion constant. One of the most reliable algorithms for this work is Dr. Provencher's CONTIN algorithm. But caution is necessary when applying size distribution analysis to correlation data, for the following reasons. Inversion of eqn. (5) in the presence of noise is an ill-posed mathematical problem. Most algorithms work reasonably well for stationary size distributions spreading over several decades in radius, as encountered in polymer studies. For tighter size distributions likely to be encountered in early aggregation stages these programs are more prone to produce artifacts. In addition, in the late

stages of aggregation, a few large clusters tend to dominate the scattered intensity, skewing the results towards large molecular weights.

In order to reduce these uncertainties in the inversion process, we are taking the following additional steps: Measurements of $G_2(\tau)$ will be taken over a range of different scattering angles (15°-150°), allowing us to probe the sample on length scales ranging from 240 nm down to 30 nm. A newer version of CONTIN uses this multiple q information to check for self-consistency in the fits. Furthermore, we plan to perform simultaneous measurements of the total scattering intensity at each angle. This provides valuable information about molecular weight distribution and deviations from simple Brownian behavior. We can also use it to check our size distributions against the corresponding intensity values.

We have performed preliminary measurements on lysozyme, which confirm that this approach is viable in our set-up. The analysis of these dynamic scattering data showed the expected q^2-dependence of the decay rate but also produced small systematic deviations from it, which we are currently exploring. The static scattering results where tainted by insufficient power stabilization on the laser employed in these test runs. Our main laser, which we just received after tube refurbishment, provides the required stabilization circuitry.

In the following months, we plan to develop and use the integrated analysis of static and dynamic light scattering data at varying scattering angles. The several hundred spectra accumulated during a typical run require a highly automated analysis procedure. Getting reliable and self-consistent results on the nucleation kinetics of lysozyme certainly justifies this effort. We hope to identify a clear signature in the scattering data, to distinguish between conditions producing craggs vs. praggs, which we feel are closely related to the colloidal aspects of these solutions.

In future work we plan to extend this approach to different protein systems. For the time being, however, we want to use lysozyme as a well characterized and studied material, in order to contrast the results of this novel approach against existing results.

3. Presentations, Publications and Other Professional Activities

Presentations

P.G. Vekilov, M. Ataka and T. Katsura, *Growth kinetics of protein crystals investigated by laser Michelson interferometry;* talk at the Conference on Protein Crystal Growth in Microgravity, Panama City, Florida, April 24, 1993.

P.G. Vekilov, M. Ataka and T. Katsura, *Interferometric studies of protein crystal growth*; invited talk at the 5-th International Conference on Crystal Growth of Biological Macromolecules, San Diego, California, August 11, 1993

P.G. Vekilov, *Dislocation source activity in growth and dissolution of crystals from solution*; talk at the 7-th Annual Alabama Materials Science Conference, Huntsville, Alabama, September 25, 1993.

L.A. Monaco, F. Rosenberger, *Growth kinetics and morphology of tetragonal lysozyme*; invited talk at the Protein Crystal Growth in Microgravity Conference, Panama City Beach, Florida, April 23-26, 1993.

L.A. Monaco, Hong Lin, A. Nadarajah, F. Rosenberger, *Convective flow effects on protein crystal growth diffraction resolution - A research plan*; The Protein Crystal Growth in Microgravity Conference, Panama City Beach, Florida, April 23-26, 1993.

L.A. Monaco, F. Rosenberger, *Kinetics and morphology of protein crystal growth*; Biology Seminar, Brookhaven National Labs, Long Island, New York, June 4, 1993.

L. Monaco, P. Vekilov, F. Rosenberger, *Kinetics, morphology and segregation in lysozyme crystallization*; invited talk at Fifth International Conference on Crystallization of Biological Macromolecules, San Diego, California, August 8-13, 1993.

L.A. Monaco, P. Vekilov, F. Rosenberger, *Kinetics, morphology, and segregation in lysozyme crystallization*; 7-th Annual Alabama Materials Science Conference, Huntsville, Alabama, September 21, 22, 1993.

Other Related Professional Activities

Franz Rosenberger has organized and chaired a session on Physics of Crystallization at the Fifth International Conference on Crystallization of Biological Macromolecules, August 8-13, 1993 in San Diego, CA. He has also been elected president of the Advisory Board for the Sixth International Conference on Crystallization of Biological Macromolecules, to be held in October 1995 in Kyoto, Japan.

The University
Of Alabama
In Huntsville

Center for Microgravity and Materials Research

Workshop on Characterization of Liquids Using Light Scattering

Thursday, July 1, 1993

11:45 Lunch in Marriott Hotel

13:00 - 15:00 Presentations in E-8, Research Institute, UAH

Prof. Harbans S. Dhadwal, Dept. of Electrical Engineering, SUNY at Stonybrook

Fiber optics systems for on-line monitoring

Dr. Martin Muschol, CMMR, UAH

Light scattering at growing melt-crystal interfaces

15:00 - 17:00 Laboratory Session with Novel Equipment, Discussion

18:00 Dinner

Friday, July 2, 1993

9:00 - 11:00 Presentations in E-8, Research Institute, UAH

Prof. William W. Wilson, Dept. of Chemistry, Mississippi State University

Predicting protein crystallization?

Dr. William V. Meyer, NASA Lewis Research Center

Advanced laser light scattering technology

12:00 Lunch

13:30 - 17:00 Laboratory Session and Discussion